Double spin-glass-like behavior and antiferromagnetic superexchange interaction between Fe^{3+} ions in α-$Ga_{2-x}Fe_xO_3$ ($0 \leq x \leq 0.4$)*

Lv Yi-Fei(吕益飞), Xiang Jian-Yong(向建勇)†, Wen Fu-Sheng(温福昇), Lv Wei-Ming(吕伟明), Hu Wen-Tao(胡文涛), and Liu Zhong-Yuan(柳忠元)

State Key Lab of Metastable Materials Science & Technology, Yanshan University, Qinhuangdao 066004, *China*

(Received 23 August 2014; revised manuscript received 13 October 2014; published online 30 January 2015)

Single phase of Fe^{3+}-doped α-$Ga_{2-x}Fe_xO_3$ (α-GF_xO, $x = 0.1$, 0.2, 0.3, 0.4) is synthesized by treating the β-$Ga_{2-x}Fe_xO_3$ (β-GF_xO) precursors at high temperatures and high pressures. Rietveld refinements of the X-ray diffraction data show that the lattice constants increase monotonically with the increase of Fe^{3+} content. Calorimetric measurements show that the temperature of the phase transition from α-GF_xO to β-GF_xO increases, while the associated enthalpy change decreases upon increasing Fe^{3+} content. The optical energy gap deduced from the reflectance measurement is found to decrease monotonically with the increase in Fe^{3+} content. From the measurements of magnetic field-dependent magnetization and temperature-dependent inverse molar susceptibility, we find that the superexchange interaction between Fe^{3+} ions is antiferromagnetic. Remnant magnetization is observed in the Fe^{3+}-doped α-GF_xO and is attributed to the spin glass in the magnetic sublattice. At high Fe^{3+} doping level ($x = 0.4$), two evident peaks are observed in the image part of the AC susceptibility χ''_{ac}. The frequency dependence in intensity of these two peaks as well as two spin freezing temperatures observed in the DC magnetization measurements of α-$GF_{0.4}O$ is suggested to be the behavior of two spin glasses.

Keywords: α-Ga_2O_3, susceptibility, superexchange interaction, spin glass

PACS: 75.30.Hx, 78.40.–q, 75.30.Cr, 75.60.Ej **DOI:** 10.1088/1674-1056/24/3/037502

1. Introduction

It is known that gallium oxide (Ga_2O_3) is an important wide band gap semiconducting material with good chemical and thermal stability. Ga_2O_3 can crystallize into different polymorphic phases such as rhombohedral α-, monoclinic β-, cubic γ- (spinel), and δ-Ga_2O_3 phases.[1] Among them, the monoclinic β-Ga_2O_3 is known to be the most stable form at ambient conditions. It undergoes phase transition from β-Ga_2O_3 to α-Ga_2O_3 upon increasing pressure.[2,3] The α- and β-Ga_2O_3 has a wide band gap of above 4 eV, which enables it to modify their properties such as transportation, photoluminescence, as well as magnetism by the incorporation of suitable ions in the Ga_2O_3 lattice.[4–9] For the β-Ga_2O_3, the Ga^{3+} ions are accommodated in non-equivalent tetrahedral and octahedral sites, preferential substitution for Ga^{3+} ions on either the tetrahedral or the octahedral sites depending on the radius of the impurity ions has been frequently observed. Consequently, the influence of the impurities on the properties of β-Ga_2O_3 could be complex.[5,7,10] In the α-Ga_2O_3, all the cations reside on the octahedral sites, and it is isostructural with the well-known hematite with a well established high ferromagnetic transition temperature of $\sim$ 670 K.[11] Thus, Fe^{3+} ions would be desirable to manipulate the magnetic properties of α-Ga_2O_3 for the practical application.

Experimental results of α-$Ga_{2-x}Fe_xO_3$ series are encouraging to achieve the non-conventional ferromagnetic semiconductor for room-temperature spintronic applications, including band gap tailoring, photoconductivity, ferromagnetism, multiferroic domain switching, and ferroelectric polarization.[12–17] However, most of previous work has been focused on the properties of α-$Ga_{2-x}Fe_xO_3$ with an Fe content x higher than 0.5. Kaneko *et al.* reported the preparation of high crystalline α-$Ga_{2-x}Fe_xO_3$ thin films ($0 \leq x \leq 2$) by mist chemical vapor deposition, and revealed that ferromagnetism occurred at a temperature of $\sim$ 110 K when $x \sim 0.5$.[4,18] Amores *et al.*[19] reported the synthesis of a solid solution of α-$Ga_{2-x}Fe_xO_3$ with $0 \leq x \leq 2$ at ambient pressure, and the obtained α phase was shown to be stable only below 400 °C. However, the solid solution is a mixture of α and β phases when the Fe content is low. The compression experiments showed that the transition of $\beta \rightarrow \alpha$ occurred at a pressure as high as 20–22 GPa at room temperature.[20] However, it has been shown that the pressure required for the stabilization of the metastable α-Ga_2O_3 can be greatly reduced at elevated temperatures.[21] So far, there are scare reports on the high-pressure synthesis and properties of Fe^{3+}-doped α-Ga_2O_3 with the doping level less than 0.5. In the present study, a single phase of Fe^{3+}-doped α-$Ga_{2-x}Fe_xO_3$ with $x \leq 0.4$ is fabricated at high temperature and high pressure to explore the

*Project supported by the National Basic Research Program of China (Grant No. 2010CB731605), the National Science Fund for Distinguished Young Scholars of China (Grant No. 51025103), the National Natural Science Foundation of China (Grant Nos. 51172198 and 51102206), the Natural Science Foundation of Hebei Province, China (Grant No. E2014203144), the Science Foundation for the Excellent Youth Scholars from Universities and Colleges of Hebei Province, China (Grant No. YQ2014009), and the Research Program of the College Science & Technology of Hebei Province, China (Grant No. QN2014047).

†Corresponding author. E-mail: jyxiang@ysu.edu.cn

© 2015 Chinese Physical Society and IOP Publishing Ltd

effect of Fe^{3+} doping on the structural, magnetic, and optical properties of α-Ga_2O_3.

2. Materials and methods

In order to synthesize the Fe^{3+}-doped α-Ga_2O_3, i.e., α-$Ga_{2-x}Fe_xO_3$ ($x \leq 0.4$) (refer to α-GF_xO thereafter), we firstly synthesized the Fe^{3+}-doped β-Ga_2O_3, i.e., β-$Ga_{2-x}Fe_xO_3$ ($x \leq 0.4$) (refer to β-GF_xO thereafter) as a starting material. The details of the preparation of β-GF_xO with $x = 0.1$, 0.2, 0.3, and 0.4 can be found elsewhere.[22] Briefly, the starting powders of β-Ga_2O_3 (99.999%, −325 mesh, Alfa Aesar) and α-Fe_2O_3 (99.99%, −325 mesh, Alfa Aesar) were mixed in the designed atomic ratio of Ga to Fe by a vario-planetary ball miller (Pulverisette 4, Fritsch, Germany) at a rotation speed of 200 RPM for 10 hours. After the milling, the obtained mixtures were dried at 90 °C for 24 hours and subsequently pressed into a pellet of 10 mm in diameter. A single phase of β-GF_xO ($x = 0.1$, 0.2, 0.3, 0.4) was then obtained after sintering in air at 1350 °C for 10 hours. The α-GF_xO ($x = 0.0$, 0.1, 0.2, 0.3, 0.4) managed to synthesize with the precursors of the as-received β-Ga_2O_3 and as-prepared bulk samples of β-GF_xO ($x = 0.1$, 0.2, 0.3, 0.4) in a single large-volume cubic anvil press under high pressure and high temperature. The precursors were inserted into the graphite furnace with a pure h-BN layer, which served as a barrier, as shown by the sample assembly in Fig. 1(d). The sample assembly was sintered under compressive pressures of 2–6 GPa and temperatures of 350–1050 °C for one hour, and then allowed to cool rapidly to room temperature.

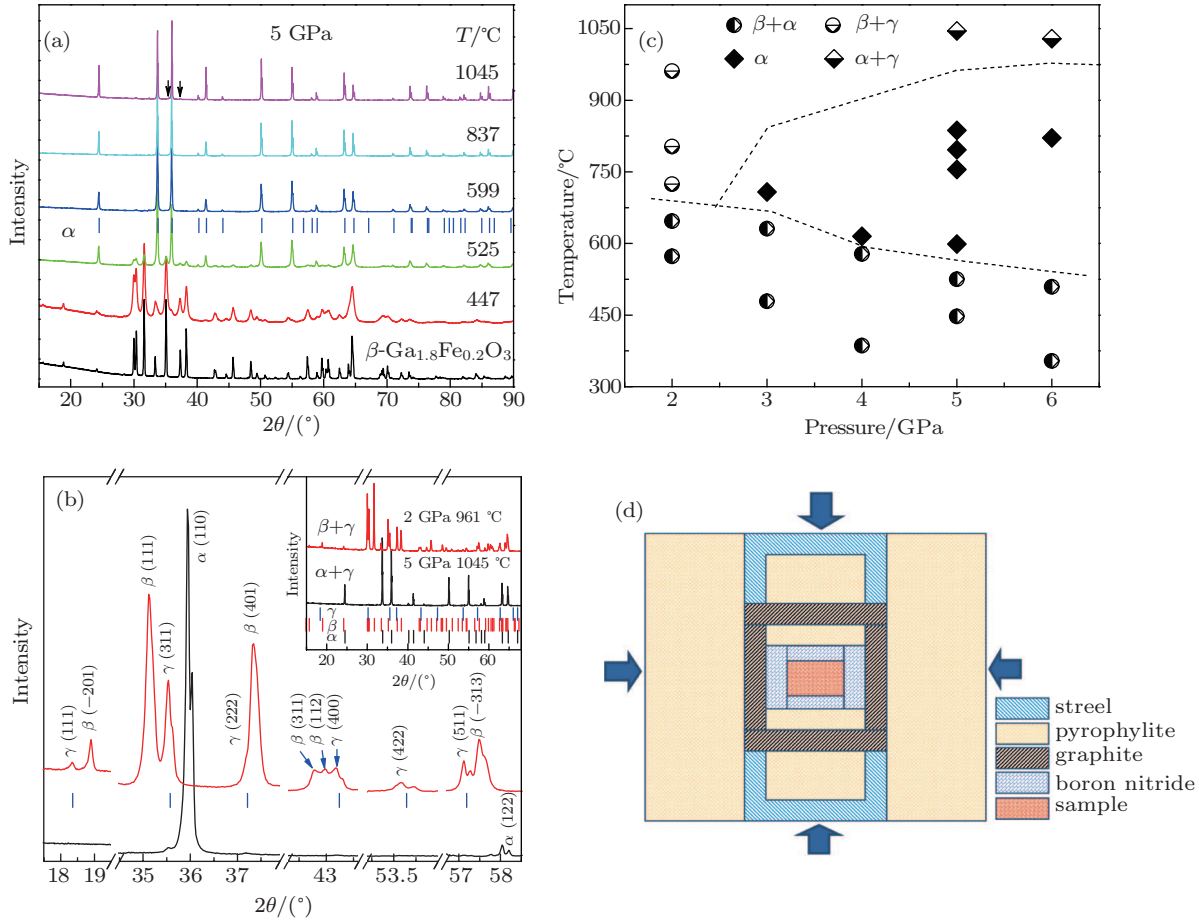


Fig. 1. (color online) (a) Powder XRD patterns for the starting β-$Ga_{1.8}Fe_{0.2}O_3$ sintered under a compressive pressure of 5 GPa and at different temperatures. The bars are the Bragg position of α-Ga_2O_3 (PDF# 06-0503). (b) Enlarged powder XRD patterns for the β-$Ga_{1.8}Fe_{0.2}O_3$ sintered at 2 GPa and 961 °C (upper, red), 5 GPa and 1045 °C (lower, black), and the inset shows the full scale of these patterns. The bars correspond to the Bragg positions of α-, β-, and spinel γ-structure with the PDF#s of 06-0503, 41-1103, and 20-0426 respectively. (c) Temperature and pressure diagram for the sintering of β-$Ga_{1.8}Fe_{0.2}O_3$. The dashed lines guide the eye. (d) An illustration of the sample assembly for the treatment at high temperature and high pressure.

The as-sintered samples were carefully polished to remove any possible contamination from the barrier, and then ground for the structure characterization, which was performed by powder X-ray diffraction (XRD) with Cu K_α radiation (PC/Dmax 2500, Rigaku, Japan). The XRD spectra were analyzed via the Rietveld refinements using software package of FullProf Suite (v2.05).[23] The Calorimetric measurements were conducted on the ground powder by a simultaneous ther-

mal analyzer (STA 449C Jupiter, Netzsch, Germany) with a heating rate of 10 °C·min^{-1} under the atmosphere of high-purity air. The magnetic measurements were carried out using a vibrating sample magnetometer attached to the PPMS (Quantum Design, USA). The diffuse reflectance was measured using a UV–Vis spectrophotometer equipped with an integrating sphere (UV-2550, Shimadzu, Japan). The reference sample is barium sulfate (Wako 1st grade, Wako Pure Chemical Industries, Ltd., Japan).

3. Results and discussion

In order to elucidate the required pressure and temperature for the preparation of single phase of Fe^{3+}-doped α-Ga_2O_3 from the starting powder of Fe^{3+}-doped β-Ga_2O_3, a concentration of 10 at% Fe^{3+} was chosen (i.e., β-$Ga_{1.8}Fe_{0.2}O_3$ or β-$GF_{0.2}O$) and treated at different temperatures and pressures. Figure 1(a) shows the collected powder XRD spectra at room temperature for the sintered β-$GF_{0.2}O$ under a compressive pressure of 5 GPa with different temperatures. With the increase in temperature, diffraction lines of β-$GF_{0.2}O$ (PDF# 41-1103) were observed to decrease in intensity and broaden in width, disappeared at ~599 °C. Bragg peaks of α-$GF_{0.2}O$ (PDF# 06-0503) were observed to appear at ~447 °C and increases in intensity upon increasing temperatures. The β-$GF_{0.2}O$ was completely transformed to α-$GF_{0.2}O$ at a temperature higher than 599 °C. The observed transition of $\beta \rightarrow \alpha$ at elevated temperatures is in good agreement with previous reports.[21] However, we find that the temperature required for the synthesis of single phase of α-$GF_{0.2}O$ is as low as ~ 600 °C, which is quite low in comparison with that reported in Ref. [21]. A new set of diffraction peaks appears beside those of the α-$GF_{0.2}O$ (Fig. 1(c)) when the temperature is increased to 1045 °C, which is close to the limitation of the safety temperature of our apparatus. These peaks coincide well with the diffraction lines of spinel-type γ-Ga_2O_3 (PDF# 20-0426), except for a downshift of the diffraction lines due to the larger radius of Fe^{3+}. Various pressures and temperatures were tried to treat the starting powder of β-$GF_{0.2}O$, and the XRD data of these samples were analyzed and summarized in Fig. 1(b). It demonstrates that the temperature window for the synthesis of single α-phase is narrowed down when decreasing the sintering pressure. By decreasing the pressure to 2 GPa, there is no single phase of α-$GF_{0.2}O$ observed, and the as-prepared sample shows a mixture of either $\beta + \alpha$ or $\beta + \gamma$.

According to the temperature–pressure (T–P) phase diagram shown in Fig. 1(b), the sintering pressure and temperature are chosen to be 5 GPa and 850 °C, respectively, for the synthesis of single phase of α-GF_xO with $x = 0$, 0.1, 0.2, 0.3, and 0.4. Figure 2(a) shows the collected powder XRD spectra at room temperature for the sintered α-GF_xO samples, confirming the single phase of corundum-type structure

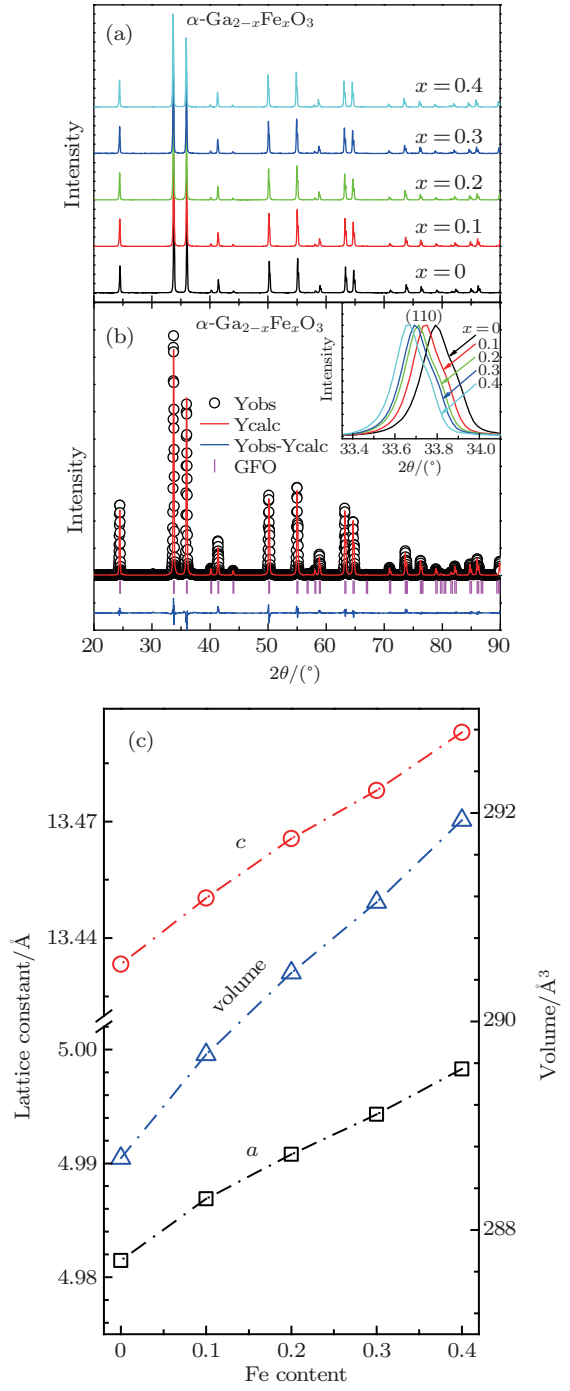


Fig. 2. (color online) (a) Powder XRD patterns for α-$Ga_{2-x}Fe_xO_3$ with $x = 0$, 0.1, 0.2, 0.3, and 0.4 synthesized at 5 GPa and temperature of 800 °C for 1 hour. (b) A typical Rietveld refinement for the as-prepared α-$Ga_{1.8}Fe_{0.2}O_3$. Empty circles represent the experimental data, and solid line is the calculated one. The curve at the bottom is the difference between the experimental and calculated data, and the vertical lines represent the Bragg positions of α-$Ga_{2-x}Fe_xO_3$ and standard silicon. Inset shows the enlarged (104) Bragg peak of α-$Ga_{2-x}Fe_xO_3$, showing the systematic shift towards the lower angle upon increasing the Fe^{3+} content. (c) Refined lattice parameters (a, c, and unit cell volume) as a function of the Fe^{3+} content for α-$Ga_{2-x}Fe_xO_3$.

of undoped and Fe^{3+}-doped samples. The enlarged diffraction peaks of (110) in the inset of Fig. 2(b) display clearly that the diffraction peaks shift consistently towards the lower angle with the increase of Fe^{3+} content, demonstrating the expansion of lattice constants induced by the successful replace-

ment of Ga^{3+} by Fe^{3+}. The Rietveld refinements with consideration of the corundum R-3c symmetry were carried out on the XRD spectra of the Fe^{3+}-doped and undoped α-Ga_2O_3. As a typical example, the experimental and calculated XRD spectra for α-$GF_{0.2}O$ are shown in Fig. 2(b). For all the synthesized samples, the calculated spectra are in a good agreement with the experimental ones, with the agreement factors of the weighted profile factor and the goodness of fitting larger than 10 and 6, respectively. For the as-prepared α-Ga_2O_3, the lattice parameters a and c, and the unit cell volume are determined to be 4.9814(5) Å, 13.4327(3) Å, and 288.671(3) $Å^3$, respectively, which are consistent with previous report.[21] The lattice constants of a and c, and the unit cell volume increase upon increasing the Fe^{3+} content (Fig. 2(c)), demonstrating the doping-induced structural expansion along the different axes.

To investigate the thermostability of sintered α-GF_xO, we employ a differential scanning calorimetry (DSC) for samples of α-GF_xO ($x = 0$, 0.1, 0.2, 0.3, 0.4) in the temperature range from room temperature to 1100 °C. No appreciable changes of the thermogravimetry (TG) signals are found over the entire temperature range for investigated samples. For the undoped and Fe^{3+}-doped α-Ga_2O_3 samples, there is only one exothermic peak observable from room temperature to 1100 °C. The exothermic peak was observed to occur at an onset and peak temperature of ~ 560 °C and ~ 594 °C respectively for the undoped α-Ga_2O_3, and they were found to shift toward higher temperature with the increase of Fe^{3+} content (Fig. 3(c)). After one thermo-cycle, XRD results show that the final product is single phase of β-GF_xO with a monoclinic structure (Fig. 3(c)). Thus, the exothermic peaks are attributed to the transition of the metastable α-GF_xO to the stable β-GF_xO. The area of the exothermic peak, which corresponds to the enthalpy change ΔH associated with the transition of α-$GF_xO \rightarrow \beta$-GF_xO, is determined to be ~–3.7 $kJ{\cdot}mol^{-1}$ for the undoped α-Ga_2O_3, being in a reasonable agreement with the theoretical expectation at 5 GPa.[24] It decreases with the increase of Fe^{3+} content (Fig. 3(b)), being indicative of the decreased energy difference between the Helmholtz free energy of β-phase and α-phase, which is consistent with the theoretical expectation.[24]

The doping of Fe atoms into the Ga sites of α-Ga_2O_3 structure is further confirmed from the absorption spectra of the samples in UV–Visible range (200–1000 nm). The required relative diffuse reflectance spectra R refering to the $BaSO_4$ standard of the undoped α-Ga_2O_3 and Fe^{3+}-doped α-GF_xO samples were converted to the Kubelka–Munk functions $F(R)$ $(= (1-R)^2/2R)$ and shown in Fig. 4(a), where $F(R)$ is proportional to the absorption coefficient.[25] For the undoped α-Ga_2O_3 sample, a strong absorption edge is observed to occur at E_g (edge) ~ 5.3 eV. With the increase of Fe^{3+}

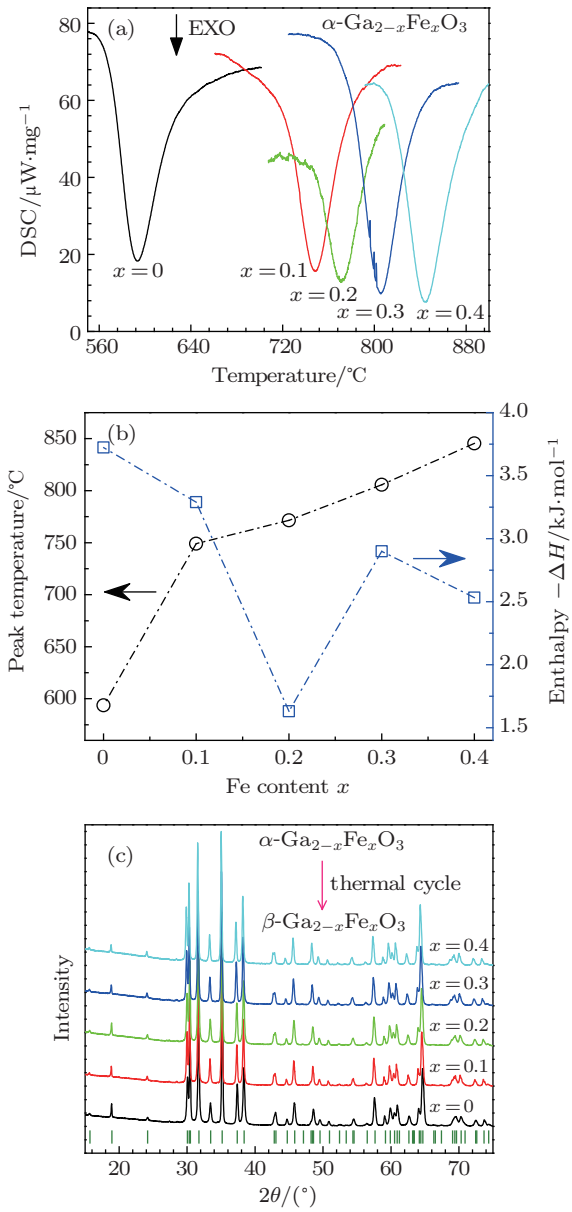


Fig. 3. (color online) (a) The DSC signals at the temperatures near the exothermic peak for powder samples of α-$Ga_{2-x}Fe_xO_3$ with $x = 0$, 0.1, 0.2, 0.3, and 0.4 synthesized at 5 GPa and temperature of 800 °C for 1 hour. The curves are shifted on the Y axis for a better view. (b) The peak temperature and integral area (associated enthalpy change ΔH) of the exothermic peak as a function of Fe content. (c) The powder XRD patterns of the products after one thermal cycle of α-$Ga_{2-x}Fe_xO_3$ ($x = 0$, 0.1, 0.2, 0.3, 0.4). The bars show the Bragg position of β-Ga_2O_3 (PDF# 41-1103).

concentration, the absorption edge shifts systematically toward lower energy (Fig. 4(b)). For the Fe^{3+}-doped α-GF_xO, a number of subspectra are observed below the absorption edge, which is consistent with the previous report.[19] In the octahedral environment of Fe^{3+} ions (i.e., FeO_6) five-fold degeneracy of d orbital splits into low-energy t_{2g} and higher-energy e_g levels. Transition of electrons between these levels contributes to absorption bands in the UV–Vis region. Among these subspectra, the bands at ~ 1.8 eV and ~ 2.6 eV are well defined and found to shift toward a lower energy with the increase of Fe^{3+} content. They are ascribed to the electronic transitions of $^6A_{1g}$ (^6S) $\rightarrow$ $^4T_{2g}$(^4G) and $^6A_1$(^6S) $\rightarrow$ $^4T_{2g}$(^4D) of Fe^{3+}

respectively, according to previous work on oxides containing Fe^{3+} and Mn^{2+} ($3d^5$).[26–28]

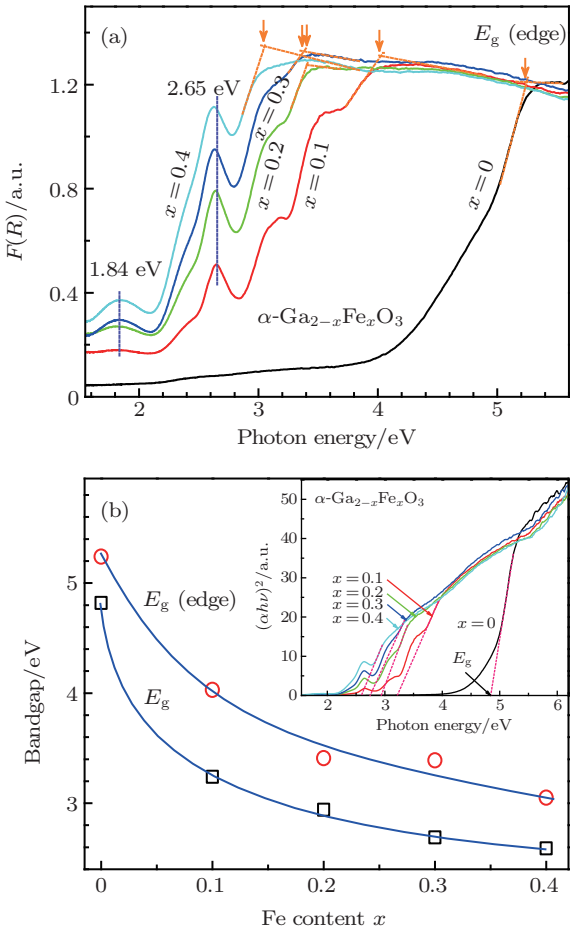


Fig. 4. (color online) Diffuse reflectance spectra of α-$Ga_{2-x}Fe_xO_3$ with $x = 0$, 0.1, 0.2, 0.3, and 0.4. (a) The Kubelka–Munk function $F(R)$, which is proportional to the absorption coefficient, converts from the relative diffuse reflectance spectra R. The downside arrows denote definition of the bandgap at the absorption edge E_g (edge). The vertical lines show the position of two absorption peaks corresponding to the d-d transition of octahedrally coordinated Fe^{3+} ions. (b) Optical bandgap E_g and E_g (edge) as a function of Fe^{3+} content. Inset is the Tauc plot of $(F(R) \times h\nu)^2$ versus $h\nu$ showing the definition of the E_g. The solid lines guide the eyes.

In order to determine the room-temperature optical bandgap (E_g) of the undoped α-Ga_2O_3 and Fe^{3+}-doped α-$Ga_{2-x}Fe_xO_3$ samples, we use the relational expression proposed by Tauc *et al.*[29] in conjunction with the Kubelka–Munk function for a semiconductor, $h\nu F(R) \propto A(h\nu - E_g)^{m/2}$, where h is the Planck constant, $h\nu$ the incident photon energy, m is related to the nature of transition and is 1 or 4 for a direct or indirect allowed transition, and A the proportional constant independent of the photon energy. For the pure α-Ga_2O_3 and α-Fe_2O_3, or Ga-doped Fe_2O_3, it was reported that the band gaps are of direct transition,[12,30,31] and we take the assumption of direct transition for the Fe^{3+}-doped α-Ga_2O_3. Therefore, the energy intercept of Tauc plot[32] of $(F(R) \times h\nu)^2$ versus $h\nu$ gives E_g for a direct allowed transition when the linear region is extrapolated to zero ordinate, as indicated in the inset of Fig. 4(b). The determined E_g for the undoped α-Ga_2O_3 is ~ 5.3 eV, being consistent with the published values of 4.9–5.6 eV.[9,30,31,33] Upon increasing the Fe^{3+} concentration, E_g is found to decrease monotonically (Fig. 4(b)), reaching a value of ~ 2.9 eV of the sample with the Fe^{3+} concentration $x = 0.4$. The decrease of optical energy gap and red shift of absorption band indirectly confirm the doping of Fe into α-Ga_2O_3 structure.

Figures 5(a)–5(d) show the DC magnetization M versus magnetic field H curves measured at different temperatures for α-GF_xO with $x = 0.1$, 0.2, 0.3, and 0.4, respectively. For the sample of α-$GF_{0.1}O$, no magnetic hysteresis is detectable (inset of Fig. 5(a)). It does not behave in a paramagnetic way at low temperature since the plot of M as a function of the ratio of H to T does not comply with the Langevin theory of paramagnetism. When the Fe^{3+} concentration x is increased to 0.2 or higher, remnant magnetization is observed (inset of Figs. 5(b)–5(d)). The slanted hysteresis diagrams of the remnant fields versus applied field are similar to ferromagnetic diagrams. However, for all the samples with the Fe^{3+} content higher than 0.2, the coercive field of ~ 10 mT and the remanence on an order of $\sim 10^{-3}\mu_B$ per Fe^{3+} ion are obtained. The hysteresis loop is reduced with increasing temperature and vanishes at ~ 30 K. Such a small magnetic moment, however, cannot be explained as a simple ferromagnetic ordering of localized spins but a frozen ferromagnetic moment in the spin-glass state.

The inset of Fig. 6 is the inverse susceptibility of χ_m^{-1} as a function of temperature for samples of α-GF_xO. In the high temperature range, χ_m^{-1} displays the linear variation with temperature in the range of 150–300 K, following the Curie–Weiss law. Moreover, the extrapolation of the fitting lines show positive intercepts, demonstrating an antiferromagnetic coupling between the Fe^{3+} ions in α-$Ga_{2-x}Fe_xO_3$.

In order to investigate the antiferromagnetic coupling in the diluted magnetic semiconductors, a modified Brillouin function is used to describe the magnetization behavior by introducing the effective temperature (T_{eff}) and the effective saturation magnetization (μ_{sat}) per magnetic ion or the effective concentration (x_{eff}) of magnetic ions.[34,35] For the Fe^{3+}-doped α-GF_xO, the modified Brillouin function.[34] $M = (xN_A\mu_{sat}/m_x)B_{5/2}(5/2g\mu_B H/k_B T_{eff})$ is used to fit the measured M versus H curves at 5 K for α-GF_xO, where $g = 2$, μ_B is the Bohr magneton, N_A and k_B are Avogadro and Boltzman constants, respectively, x is the Fe^{3+} concentration, and m_x is the molar mass of α-GF_xO. $T_{eff} = T + T_0$ and μ_{sat} are used as the fitting parameters, which can be used to reflect the antiferromagnetic superexchange interaction between the Fe^{3+} ions.[35] Figure 7 shows that the fitting is in good agreement with the measured M versus H curves at 5 K for α-GF_xO, and the inset shows the obtained T_0 and μ_{sat} as a function of the

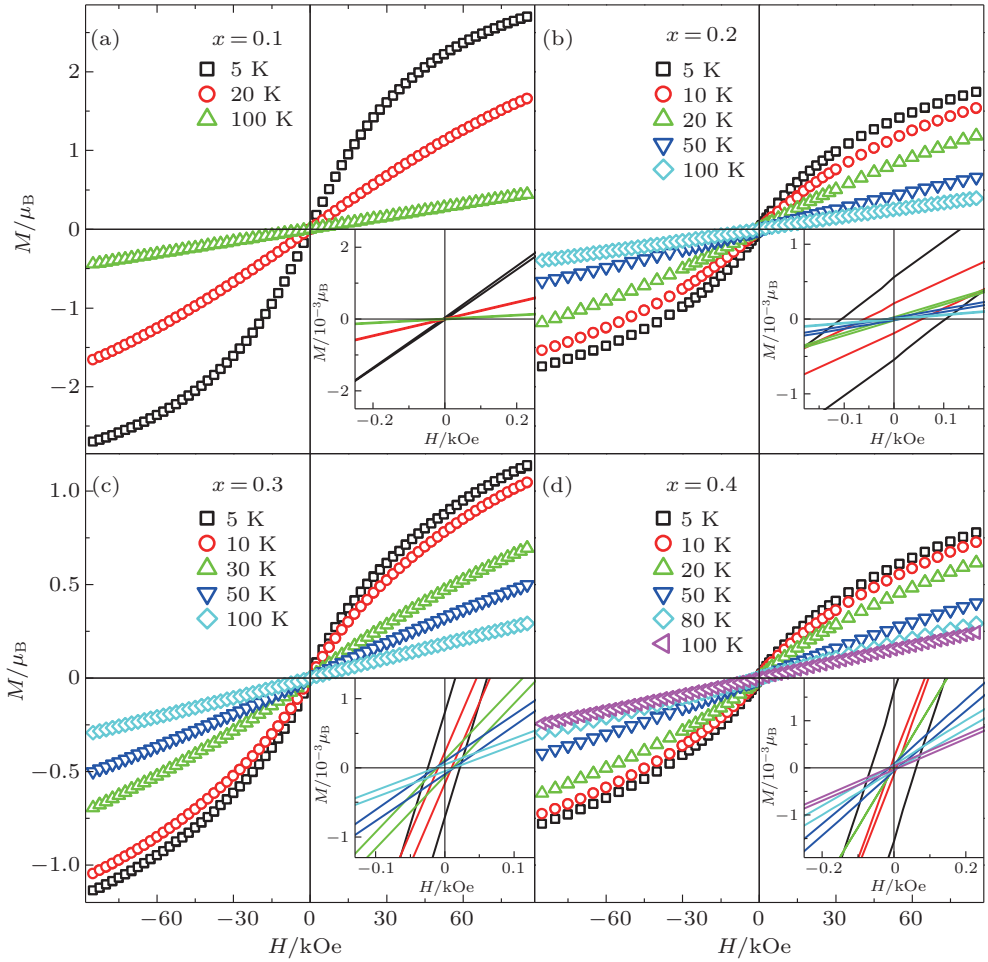


Fig. 5. (color online) (a) Magnetization as a function of the magnetic field for the sample α-$Ga_{2-x}Fe_xO_3$ at different temperatures. (a) α-$GF_{0.1}O$ at 5, 20, and 100 K. (b) α-$GF_{0.2}O$ at 5, 10, 20, 50, and 100 K. (c) α-$GF_{0.3}O$ at 5, 10, 30, 50, and 100 K. (d) α-$GF_{0.4}O$ at 5, 10, 20, 50, 80, and 100 K. Inset is the enlarged plots of M–H loops of the corresponded temperatures.

Fe^{3+} content x. In the sublattice of α-GF_xO, if two Fe^{3+} ions via an intermediate oxygen ion forms an antiferromagnetic pair of Fe^{3+}–O–Fe^{3+}, their moments can be cancelled and make no contribution to the measured magnetization. Only the uncoupled Fe^{3+} ions can be aligned in the applied magnetic field, according to the Brillouin function with $T_{\rm eff}$ greater than the real temperature T or positive T_0. Thus, the obtained value of $\mu_{\rm sat}$ smaller than $5.92\mu_{\rm B}$ and the positive T_0 indicate that a fraction of Fe^{3+} ions form the Fe^{3+}–O–Fe^{3+} pairs with antiferromagnetic superexchange interaction. At 5 K, the saturation cannot be obtained at the magnetic field of 85 kOe. Thus, the measured magnetic moment per Fe^{3+} ion at 5 K and 85 kOe is smaller than the effective saturation moment $\mu_{\rm sat}$ obtained from the fitting, but they show similar dependence on the Fe^{3+} content x. With the increase of the Fe^{3+} content x, the decrease of $\mu_{\rm sat}$ is suggestive of the formation of more Fe^{3+}–O–Fe^{3+} pairs with the antiferromagnetic superexchange interaction. Moreover, T_0 is found to increase with the increase of Fe^{3+} content x. These behaviors of the obtained $\mu_{\rm sat}$ and T_0 indicate that the antiferromagnetic interaction between the magnetic ions becomes stronger with the increase of the Fe^{3+} content.[35]

Figure 6 shows the temperature dependence of zero-field cooling (ZFC) and field cooling (FC) of the DC magnetization measured in the magnetic field of 100 Oe for α-GF_xO with $x = 0.1$, 0.2, 0.3, and 0.4. For the sample of α-$GaF_{0.1}O$, the ZFC curve coincides with the ZFC curve. Irreversible magnetization (splitting of ZFC and FC magnetization) is observed to occur at the temperature of $\sim$ 33 K for $x = 0.2$ and shifts slightly towards higher temperature with the increase of Fe^{3+} content, and at $\sim$ 42 K when $x = 0.4$. This is consistent with the previous reports that the spin freezing temperature increases with the increased concentration magnetic ions.[36] In addition, for the sample of $GF_{0.4}O$, a second splitting of ZFC and FC magnetization is observed to occur at a lower temperature of $\sim$ 7.2 K.

Temperature-dependent AC susceptibility is measured to investigate the dynamics of the magnetization of the spontaneous magnetic behaviors of the Fe^{3+}-doped α-GF_xO. Figure 7 shows the real part $\chi'_{\rm ac}$ and imaginary part $\chi''_{\rm ac}$ of AC susceptibility $\chi_{\rm ac}$ measured at the temperatures of 5–300 K and frequencies of 0.5, 0.9, 1.0, 5, and 7 kHz for α-GF_xO

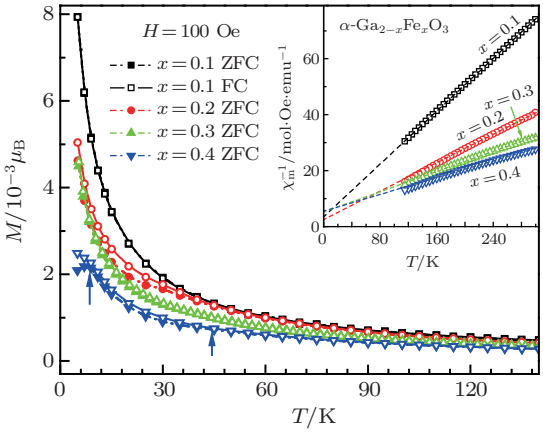


Fig. 6. (color online) Zero-field cooling (ZFC, solid symbols) and field cooling (FC, empty symbols) of the DC magnetization as a function of temperature from 5 to 140 K for α-$Ga_{2-x}Fe_xO_3$ with $x = 0.1$, 0.2, 0.3, and 0.4. A magnetic field of 100 Oe is applied for all the measurements. Arrows denote the definition of the temperatures where irreversible magnetization occurs. Inset is the inverse molar susceptibility as a function of temperature for α-$Ga_{2-x}Fe_xO_3$ with $x = 0.1$, 0.2, 0.3, and 0.4. The dash lines are the linear fitting.

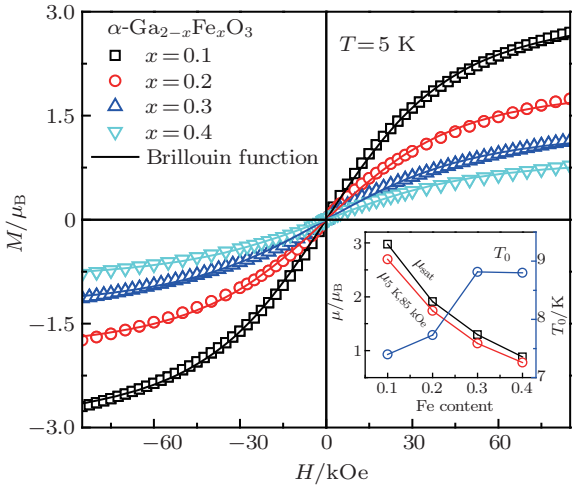


Fig. 7. (color online) Magnetization as a function of the magnetic field measured at 5 K for α-$Ga_{2-x}Fe_xO_3$ with $x = 0.1$, 0.2, 0.3, and 0.4. Solid lines are the fittings to the modified Brillouin function. Inset is the measured magnetic moment per Fe^{3+} ion at 85 kOe and 5 K, the calculated saturation magnetic moment per Fe^{3+} ion, and the temperature T_0 as a function of the Fe^{3+} content.

($x = 0.1$, 0.2, 0.3, 0.4). The real part χ'_{ac} at 5 K decreases in amplitude with the increase of Fe^{3+} content (top panels of Figs. 8(a)–8(d)). Small shoulders of χ'_{ac} could be distinguished at the temperature when the maxima of χ''_{ac} occurs, and show very weak frequency dependence. For sample $GF_{0.1}O$, noticeable anomalies of χ''_{ac} are observed to occur at a temperature of $\sim$ 33 K when the frequency is higher than 1 kHz (Fig. 8(a)), though no evident splitting of the ZFC and FC magnetization is observed. As the Fe^{3+} content increases to $x = 0.2$, as shown in the inset of bottom panel of Fig. 8(b) for sample $GF_{0.2}O$, noticeable anomalies occur in χ''_{ac} at $\sim$ 30 K, which is close to the spin freezing temperature of the sample α-$GF_{0.2}O$ (Fig. 6). The anomaly in χ''_{ac} shows a clear frequency dependence in amplitude and a very weak frequency dependence in temperature, which can be attributed to the entrance of spin glass.[37–39] With the increase of Fe^{3+} content, the anomaly in χ''_{ac} measured at 7 kHz is found to decrease in amplitude and shift toward higher temperatures. For the sample $GF_{0.3}O$, the curves of χ''_{ac} at all the frequencies turn to increase rapidly at $\sim$ 8 K with the decrease of temperature (bottom panel of Fig. 8(c)), and presumably the maxima of χ''_{ac} occur at a temperature below 5 K. This is more evident for the sample $GF_{0.4}O$ (bottom panel of Fig. 8(d)), clear anomalies of χ'_{ac} and χ''_{ac} are observed to occur at a lower temperature of $\sim$ 7.2 K, where the splitting of ZFC and FC magnetization is also observed to occur (Fig. 6). In addition, the anomaly increases in amplitude and shifts slightly to higher temperatures with the increase of frequency. The occurrence of two distinct peaks in χ''_{ac} as well as two spin freezing temperatures observed in the DC magnetization of $GF_{0.4}O$ indicate the existence of two distinct spin glass states as suggested[40–43] and also confirm the two phase transition temperatures at $\sim$ 7.2 K and 40 K.

According to previous work on the anisotropic spin-glasses,.[42,44–46] the above-mentioned two spin-glasses transitions observed from paramagnetic state could occur in the presence of random exchange interaction and local uniaxial magnetic anisotropy. On one hand, the α-Ga_2O_3 is isostructrual with α-Fe_2O_3, and Ga^{3+} ions can be unlimitedly substituted by Fe^{3+} ions with very limited distortion to the crystal structure due to the small difference of the radius of Ga^{3+} ion and Fe^{3+} ion. In α-Fe_2O_3, it is well known that there are two magnetic sublattices with equal moment that interact via an antiferromagnetic coupling, and a small canting of the two sublattices results in weak ferromagnetism between the Morin temperature and the Néel temperature.[47,48] Thus, it is believed that the incorporated Fe^{3+} ions on two sublattices are diluted by the nonmagnetic Ga^{3+} ions and are randomly distributed over the corresponding sublattices. Although they are randomly coupled through the AFM superexchange interactions, these bonds do not make up a periodic structure, and long-range AFM order cannot set in among the moments located in the two sublattices. On the other hand, it was suggested that the easy axis of magnetic anisotropy arises from the magnetic dipole anisotropy and single-ion anisotropy changes during the spin reorientation at the Morin temperature.[47] Such an anisotropy also existed and resulted in a large coercivity in Fe-doped α-Ga_2O_3.[13] It is shown here that the temperatures associated with spin temperature increase with the increase of Fe^{3+} ion concentration. We believe that two spin-glasses behavior could occur and be more profound in α-GF_xO with the Fe^{3+} concentration x higher than 0.4, though ferromagnetic ordering was reported to form at $x \approx 0.5$.[4,18] A detailed investigation of the spin dynamics in the Fe^{3+}-doped α-Ga_2O_3 ($0.4 \leq x \leq 0.6$) will be discussed.

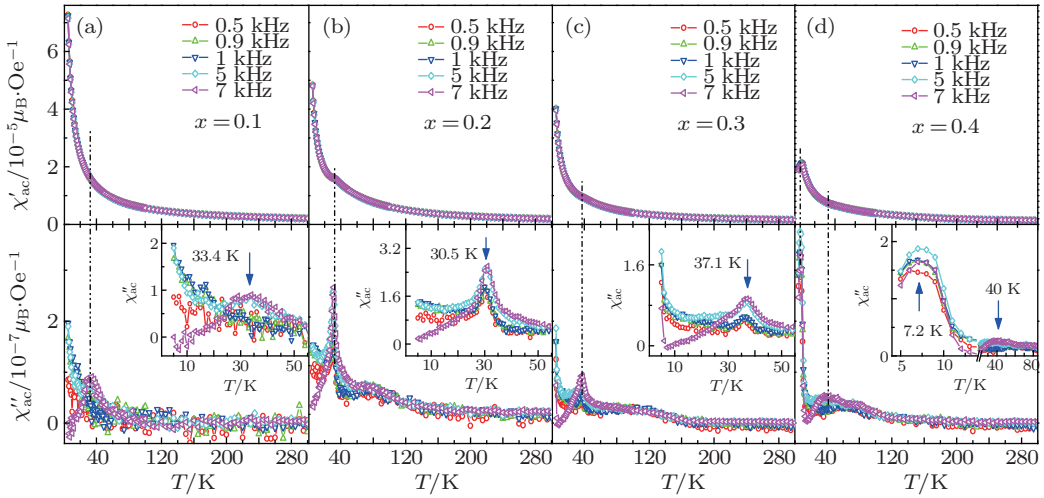


Fig. 8. (color online) The AC susceptibility χ_{ac} measured in a zero dc magnetic field as a function of temperature at the frequencies of 0.5, 0.9, 1, 5, and 7 kHz for α-$Ga_{2-x}Fe_xO_3$ with (a) $x = 0.1$, (b) 0.2, (b) 0.3, and (d) 0.4. The top and bottom panel of each figure correspond to the real (χ'_{ac}) and imaginary (χ_{ac}) parts of χ_{ac}. The AC driving magnetic field has an amplitude of 5 Oe. Insets of the bottom panel show χ_{ac} in low temperature range, and arrows show the peak temperature of the corresponding samples.

4. Summary

In summary, a series of single-phase Fe^{3+}-doped wide gap oxide of α-Ga_2O_3, i.e., α-$Ga_{2-x}Fe_xO_3$ with $x = 0.1$, 0.2, 0.3, and 0.4, has been successfully fabricated via treating single phase of β-$Ga_{2-x}Fe_xO_3$ at high temperature and high pressure. Rietveld refinements of the X-ray diffraction data show that the lattice constants increase monotonically with the increase of Fe^{3+} content. Calorimetric measurements show that the temperature of the phase transition from α-GF_xO to β-GF_xO increases, while the associated enthalpy change decreases upon increasing Fe^{3+} content. The optical energy gap deduced from the reflectance measurement and the absorption edge are found to decrease monotonically with the increase of Fe^{3+} content. Below the E_g edge, optical absorption structures are observed to occur at ~ 1.8 and ~ 2.6 eV, which are attributed to the d–d transitions of the crystal-field splitting of $3d^5$ multiplets of the octahedrally coordinated Fe^{3+} ion. From the analyses of the magnetic measurements, it is found that a fraction of the doped Fe^{3+} ions form the Fe^{3+}–O–Fe^{3+} pairs with antiferromagnetic superexchange interaction. The Fe^{3+}–O–Fe^{3+} pairs should increase in number with the increase of Fe^{3+} content, leading to the observed reduction in the measured magnetic moment per Fe^{3+} ion. The two distinct anomalies in the imaginary part of the ac susceptibility χ''_{ac} accompanied with two splitting of ZFC and FC curves occur in Fe^{3+}-doped α-Ga_2O_3. This behavior is suggested to be because the successive transition of two spin glasses arises from the magnetic anisotropy.

References

[1] Roy R 1952 *Journal of the American Chemical Society* **74** 4
[2] Machon D 2006 *Phys. Rev. B* **2006** 9
[3] Yusa H 2008 *Phys. Rev. B* **77** 9
[4] Kaneko K, Kakeya I, Komori S and Fujita S 2013 *J. Appl. Phys.* **113**
[5] Hojo H, Fujita K, Tanaka K and Hirao K 2004 *Ferromagnetism in Fe-doped β-Ga_2O_3 Prepared by a Solid State Reaction. MRS Proceedings* (Cambridge: Cambridge University Press) p. I4.25
[6] Kim I G, Yeom T H, Lee S H, Yu Y M, Shin H W and Choh S H 2001 *J. Appl. Phys.* **89** 4470
[7] Lee S W, Ryu Y G, Ahn G Y, Park S I and Kim C S 2004 *Phys. Stat. Sol.* **1** 3550
[8] López I, Utrilla A D, Nogales E, Méndez B, Piqueras J, Peche A, Ramírez-Castellanos J and González-Calbet J M 2012 *J. Phys. Chem. C* **116** 3935
[9] Lovejoy T C, Chen R, Yitamben E N, Shutthanadan V, Heald S M, Villora E G, Shimamura K, Zheng S, Dunham S T, Ohuchi F S and Olmstead M A 2012 *J. Appl. Phys.* **111** 123716
[10] Song Y P, Wang P W, Xu X Y, Wang Z, Li G H and Yu D P 2006 *Physica E* **31** 67
[11] Pickart S J, Nathans R and Alperin H A 1964 *J. Phys. France* **25** 542
[12] Naresh N 2011 *AIP Adv.* **1** 12
[13] Wang N 2011 *Solid State Commun.* **151** 4
[14] Wang N 2010 *J. Magn. Magn. Mater.* **322** 6
[15] Eerenstein W 2006 *Nature* **442** 7
[16] Yan L 2009 *J. Mater. Sci.* **44** 15
[17] Arima T 2004 *Phys. Rev. B* **70** 8
[18] Kaneko K 2009 *Appl. Phys. Express* **2** 3
[19] Amores J M G 2001 *J. Mater. Chem.* **11** 7
[20] Machon D 2006 *Phys. Rev. B* **73** 9
[21] Marezio M 1967 *J. Chem. Phys.* **46** 4
[22] Lv Y F, Xiang J Y, Wen F S, Lv W M, Hu W T and Liu Z Y 2015 *J. Magn. Magn. Mater.* **377** 460
[23] Rodríguez-Carvajal J 2001 *IUCr Newsletter* **26** 8
[24] Yoshioka S 2007 *J. Phys. Condens. Matter* **19** 12
[25] Kortüm G, Braun W and Herzog G 1963 *Angewandte Chemie International Edition in English* **2** 333
[26] Noksha O N and Grum-Grzhimailo S V 1972 *Studies of the Optical Spectra of Crystals with Iron Group Ions at Room and Low Temperatures* (Moscow: Nauka)
[27] Krebs J J and Maisch W G 1971 *Phys. Rev. B* **4** 757
[28] Kim K J and Park Y R 2004 *J. Appl. Phys.* **96** 4150
[29] Tauc J, Grigorovici R and Vancu A 1966 *Phys. Stat. Sol. (b)* **15** 627
[30] Janowitz C, Scherer V, Mohamed M, Krapf A, Dwelk H, Manzke R, Galazka Z, Uecker R, Irmscher K and Fornari R 2011 *New J. Phys.* **13** 085014
[31] Mohamed M, Janowitz C, Unger I, Manzke R, Galazka Z, Uecker R, Fornari R, Weber J, Varley J and van de Walle C 2010 *Appl. Phys. Lett.* **97** 211903
[32] Tauc J 1968 *Mater. Res. Bull.* **3** 37
[33] Gilbert B, Frandsen C, Maxey E R and Sherman D M 2009 *Phys. Rev. B* **79** 035108
[34] Gaj J A, Planel R and Fishman G 1979 *Solid State Commun.* **29** 435
[35] Zając M, Gosk J, Kamińska M, Twardowski A, Szyszko T and Podsiadło S 2001 *Appl. Phys. Lett.* **79** 2432

[36] Dupuis V 2001 *Phys. Rev. B* **64** 7

[37] Galazka R R 1980 *Phys. Rev. B* **22** 12

[38] Mulder C A M 1981 *Phys. Rev. B* **23** 13

[39] Aeppli G, Shapiro S M, Birgeneau R J and Chen H S 1983 *Phys. Rev. B* **28** 5160

[40] Li B, Zhang X, Tian J and Zhang J 2011 *Chem. Commun.* **47** 1737

[41] Noguchi S, Okuda K, Abliz M, Goto K, Kindo K, Haga Y, Yamamoto E and Onuki Y 1998 *Physica B* **246** 4

[42] Murayama S, Yokosawa K, Miyako Y and Wassermann E F 1986 *Phys. Rev. Lett.* **57** 4

[43] Datta T, Thornberry D, Jones Jr E R and Ledbetter H M 1984 *Solid State Commun.* **52** 515

[44] Cragg D M and Sherrington D 1982 *Phys. Rev. Lett.* **49** 1190

[45] Yeshurun Y and Sompolinsky H 1985 *Phys. Rev. B* **31** 3191

[46] Hiroi M, Rokkaku T, Matsuda K, Hisamatsu T, Shigeta I, Ito M, Sakon T, Koyama K, Watanabe K, Nakamura S, Nojima T, Nakano T, Chen L, Fujiwara T, Uwatoko Y, Manaka H and Terada N 2009 *Phys. Rev. B* **79** 224423

[47] Besser P J 1967 *Phys. Rev.* **153** 11

[48] Droubay T, Rosso K M, Heald S M, McCready D E, Wang C M and Chambers S A 2007 *Phys. Rev. B* **75** 104412